LETTER

doi:10.1038/nature17140

The host galaxy of a fast radio burst

E. F. Keane[1,2,3], S. Johnston[4], S. Bhandari[2,3], E. Barr[2], N. D. R. Bhat[3,5], M. Burgay[6], M. Caleb[2,3,7], C. Flynn[2,3], A. Jameson[2,3], M. Kramer[8,9], E. Petroff[2,3,4], A. Possenti[6], W. van Straten[2], M. Bailes[2,3], S. Burke-Spolaor[10], R. P. Eatough[8], B. W. Stappers[9], T. Totani[11], M. Honma[12,13], H. Furusawa[12], T. Hattori[14], T. Morokuma[15,16], Y. Niino[12], H. Sugai[16], T. Terai[14], N. Tominaga[16,17], S. Yamasaki[11], N. Yasuda[16], R. Allen[2], J. Cooke[2,3], J. Jencson[18], M. M. Kasliwal[18], D. L. Kaplan[19], S. J. Tingay[3,5], A. Williams[5], R. Wayth[3,5], P. Chandra[20], D. Perrodin[6], M. Berezina[8], M. Mickaliger[9] & C. Bassa[21]

In recent years, millisecond-duration radio signals originating in distant galaxies appear to have been discovered in the so-called fast radio bursts[1–9]. These signals are dispersed according to a precise physical law and this dispersion is a key observable quantity, which, in tandem with a redshift measurement, can be used for fundamental physical investigations[10,11]. Every fast radio burst has a dispersion measurement, but none before now have had a redshift measurement, because of the difficulty in pinpointing their celestial coordinates. Here we report the discovery of a fast radio burst and the identification of a fading radio transient lasting ∼6 days after the event, which we use to identify the host galaxy; we measure the galaxy's redshift to be $z = 0.492 \pm 0.008$. The dispersion measure and redshift, in combination, provide a direct measurement of the cosmic density of ionized baryons in the intergalactic medium of $\Omega_{\rm IGM} = 4.9 \pm 1.3$ per cent, in agreement with the expectation from the Wilkinson Microwave Anisotropy Probe[12], and including all of the so-called 'missing baryons'. The ∼6-day radio transient is largely consistent with the radio afterglow of a short γ-ray burst[13], and its existence and timescale do not support progenitor models such as giant pulses from pulsars, and supernovae. This contrasts with the interpretation[8] of another recently discovered fast radio burst, suggesting that there are at least two classes of bursts.

As part of the SUrvey for Pulsars and Extragalactic Radio Bursts (SUPERB) project at the Parkes radio telescope, we perform real-time searches of the sky at high time resolution (see Methods). On 2015 April 18 UTC we detected a fast radio burst (FRB) which we refer to as FRB 150418. Its dispersion measure (DM) is 776.2(5) $\rm cm^{-3}\,pc$, which is 4.1 times the maximum Galactic contribution expected from this line of sight through the Milky Way[14]. (Throughout, the figure in parentheses indicates the uncertainty in the last digit.) The UTC at which the FRB was detected is 04:29:07.056 at 1,382 MHz, or 04:29:05.370 at infinite frequency with the dispersion delay removed (Fig. 1). The observed pulse width is 0.8 ± 0.3 ms, consistent with dispersion smearing due to the finite frequency resolution of the spectrometer, indicating that the intrinsic width is unresolved. No scattering is evident, consistent with the expected contribution from the Galaxy, which is $\ll$1 ms at this latitude[15]. The linear polarization is not large at 8.5 ± 1.5% and the circular polarization is consistent with zero. Given the low level of linear polarization the rotation measure is not known precisely and is $36 \pm 52\,\rm rad\,m^{-2}$. In 13 h of follow-up observations no repeat burst was detected (see Methods).

Upon detection of FRB 150418 at Parkes, a network of telescopes was triggered across a wide range of wavelengths (see Methods). Beginning two hours after the FRB, observations with the Australia Telescope Compact Array (ATCA) were carried out at 5.5 GHz and 7.5 GHz, identifying two variable compact sources. One of the variable sources is consistent with a GHz-peaked-spectrum source, with a positive spectral index, as previously identified in observations at these frequencies[16]. The other variable source (right ascension, RA 07 h 16 min 34.6 s; declination, dec. −19° 00′ 40″), offset by 1.944 arcmin from the centre of the Parkes beam, was seen at 5.5 GHz at a brightness of 0.27(5) mJy per beam just 2 h after the FRB. The source was then seen to fade over subsequent epochs, settling at a brightness of ∼0.09(2) mJy per beam (Fig. 2). The source is also seen at 7.5 GHz at 0.18(3) mJy per beam in the first epoch but subsequently not detected. These observations indicate a ∼6-day transient with a negative spectral index; we obtain $\alpha = -1.37$ in the first epoch, for a power-law spectrum of the form $F_\nu \propto \nu^\alpha$. The subsequent quiescent level is consistent with the level expected[17] from an early-type galaxy at $z \approx 0.5$. To estimate the likelihood that this transient could occur by chance we consider the results of radio imaging surveys (see Methods). By comparing to a recent survey with the Very Large Array[18] in the 2–4 GHz band, we expect a 95% (99%) confidence upper limit of <0.001 (<0.002) such transients to occur in the ATCA observations of the FRB field, or equivalently an upper limit chance coincidence probability of <0.1% (<0.2%). We find that the detection of a fading transient source is therefore sufficiently rare that we conclude that it is the afterglow from the FRB event.

We obtained optical observations of the field using Suprime-Cam on the 8.2-m Subaru Telescope on 2015 April 19 and April 20. From these images, we identify a source within the ∼1-arcsec positional uncertainty derived from the ATCA image (Fig. 3). The source is seen to be a galaxy with a half-light radius of 1.4 ± 0.2 arcsec with a surface brightness profile well fitted by de Vaucouleurs' law (see Methods), thus consistent with being an elliptical galaxy. In addition to the Subaru r' and i' band photometry, we obtained J, H and $K_{\rm s}$ band photometry with the Wide-field Infrared Camera on the Palomar 200″ telescope. The source is also detected in the WISE W1 and W2 filters, enabling a seven-band spectral energy distribution fit (see Extended Data Fig. 1) and the determination of a photometric redshift of $0.48 < z < 0.56$ (68% confidence). To confirm this redshift, we performed a 3-h spectroscopic observation in good seeing conditions (full-width at half-maximum,

[1]Square Kilometre Array Organisation, Jodrell Bank Observatory, SK11 9DL, UK. [2]Centre for Astrophysics and Supercomputing, Swinburne University of Technology, Mail H29, PO Box 218, Victoria 3122, Australia. [3]Australian Research Council Centre of Excellence for All-sky Astrophysics (CAASTRO), Australia. [4]Commonwealth Science and Industrial Research Organisation (CSIRO), Astronomy and Space Science, Australia Telescope National Facility, PO Box 76, Epping, New South Wales 1710, Australia. [5]International Centre for Radio Astronomy Research, Curtin University, Bentley, Western Australia 6102, Australia. [6]Instituto Nazionale di Astrofisica (INAF)—Osservatorio Astronomico di Cagliari, Via della Scienza 5, I-09047 Selargius (CA), Italy. [7]Research School of Astronomy and Astrophysics, Australian National University, Canberra, Australian Capital Territory 2611, Australia. [8]Max-Planck-Institut für Radioastronomie (MPIfR), Auf dem Hügel 69, D-53121 Bonn, Germany. [9]Jodrell Bank Centre for Astrophysics, School of Physics and Astronomy, University of Manchester, Manchester M13 9PL, UK. [10]National Radio Astronomy Observatory, Socorro, New Mexico, USA. [11]Department of Astronomy, the University of Tokyo, Hongo, Tokyo 113-0033, Japan. [12]National Astronomical Observatory of Japan, 2 Chome-21-1 Osawa, Mitaka, Tokyo 181-8588, Japan. [13]Department of Astronomical Science, SOKENDAI (Graduate University for the Advanced Study), Osawa, Mitaka 181-8588, Japan. [14]Subaru Telescope, National Astronomical Observatory of Japan, 650 North A'ohoku Place, Hilo, Hawaii 96720, USA. [15]Institute of Astronomy, Graduate School of Science, University of Tokyo, 2-21-1 Osawa, Mitaka, Tokyo 181-0015, Japan. [16]Kavli Institute for the Physics and Mathematics of the Universe (WPI), Institutes for Advanced Study, University of Tokyo, Kashiwa, Chiba 277-8583, Japan. [17]Department of Physics, Faculty of Science and Engineering, Konan University, 8-9-1 Okamoto, Kobe, Hyogo 658-8501, Japan. [18]Cahill Center for Astrophysics, California Institute of Technology, 1200 East California Boulevard, Pasadena, California 91125, USA. [19]Department of Physics, University of Wisconsin-Milwaukee, Milwaukee, Wisconsin 53201, USA. [20]National Centre for Radio Astrophysics, Tata Institute of Fundamental Research, Pune University Campus, Ganeshkhind, Pune 411 007, India. [21]ASTRON, the Netherlands Institute for Radio Astronomy, Postbus 2, NL-7990 AA Dwingeloo, The Netherlands.

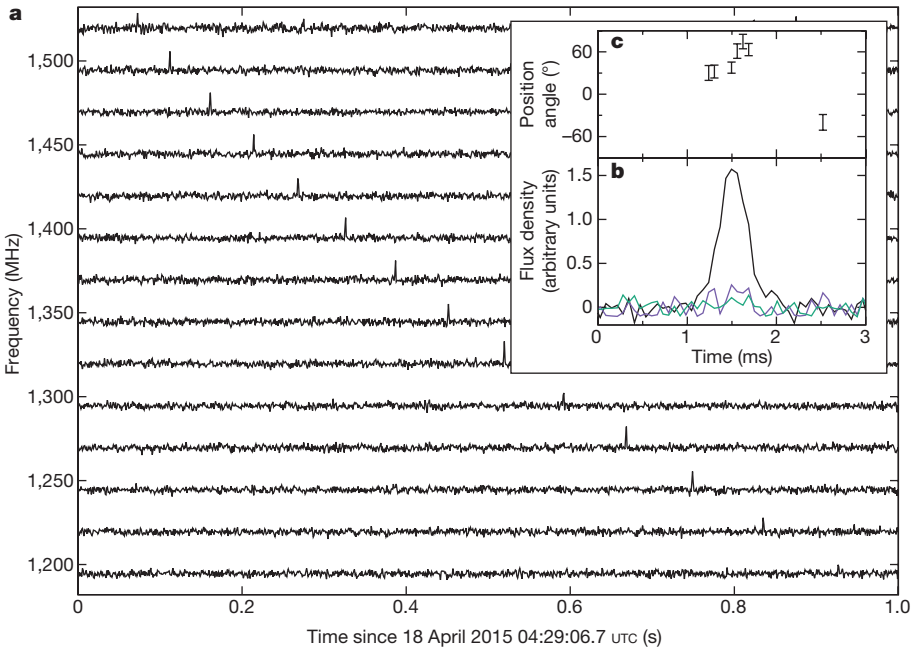

Figure 1 | The FRB 150418 radio signal. **a**, A waterfall plot of the FRB signal with 15 frequency sub-bands across the Parkes observing bandwidth, showing the characteristic quadratic time–frequency sweep. To increase the signal-to-noise ratio, the time resolution is reduced by a factor of 14 from the raw 64-μs value. **b**, The pulse profile of the FRB signal with the total intensity, linear and circular polarization flux densities shown as black, purple and green lines respectively. **c**, The polarization position angle is shown with 1σ error bars, for each 64-μs time sample where the linear polarization was greater than twice the uncertainty in the linear polarization.

FWHM ≈ 0.8 arcsec) using the Faint Object Camera and Spectrograph (FOCAS) on Subaru on 2015 November 03. This yielded a spectrum consistent with a reddened elliptical galaxy at $z = 0.492 \pm 0.008$ (Fig. 3). An earlier 1-h observation, on a night which was not spectrophotometric, using the Deep Imaging Multi-Object Spectrograph (DEIMOS) on the Keck telescope, was also taken and found to be consistent with the Subaru result.

Dispersion in the intergalactic medium is related to the cosmic density of ionized baryons $\Omega_{\rm IGM}$ and the redshift[19,20] according to the following expression:

$$\mathrm{DM_{IGM}} = \frac{3cH_0\Omega_{\rm IGM}}{8\pi G m_{\rm p}} \int_0^z \frac{(1+z')f_{\rm e}(z')\mathrm{d}z'}{[(1+z')^3\Omega_{\rm m}+\Omega_\Lambda]^{0.5}} \quad (1)$$

Here, we take $\mathrm{DM_{IGM}} = \mathrm{DM_{FRB}} - \mathrm{DM_{MW}} - \mathrm{DM_{halo}} - \mathrm{DM_{host}}(1+z)^{-1}$ (see Methods). It is appropriate to account for a Milky Way halo contribution[21] of $\mathrm{DM_{halo}} = 30\,\mathrm{cm^{-3}\,pc}$ and we derive $189\,\mathrm{cm^{-3}\,pc}$ for $\mathrm{DM_{MW}}$ (the DM for the rest of the Milky Way, excluding its halo, that is, the non-dark-matter component of the Milky Way) from the NE2001 Galactic electron density model[14]. An elliptical galaxy can be modelled[22] with a modified version of NE2001 with an average rest-frame value of $\sim 37\,\mathrm{cm^{-3}\,pc}$. The NE2001 components are uncertain at the 20% level[14], and there is an additional uncertainty of $\sim 100\,\mathrm{cm^{-3}\,pc}$ owing to line-of-sight inhomogeneities in the intergalactic medium[10]. We therefore obtain:

$$\Omega_{\rm IGM} = \left(\frac{0.88}{f_{\rm e}}\right) 0.049 \pm 0.013 \quad (2)$$

The ionization factor is $f_{\rm e} = 1$ for fully ionized hydrogen, whereas allowing for a helium abundance of 25%, $f_{\rm e} = 0.88$ is appropriate[20].

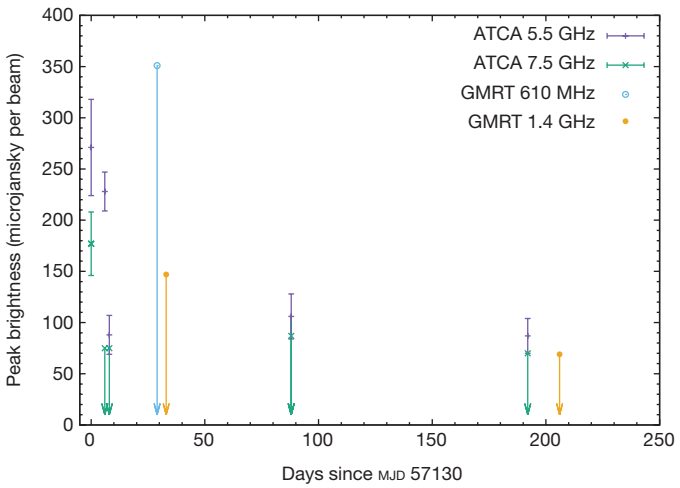

Figure 2 | The FRB host galaxy radio light curve . Detections have 1σ error bars, and 3σ upper limits are indicated with arrows. The afterglow event appears to last ~6 days, after which time the brightness settles at the quiescent level for the galaxy. Here MJD denotes modified Julian day.

Table 1 | Summary of FRB 150418 observed and derived properties

Event time at 1,382 MHz	2015 April 18 04:29:07.056 UTC
Event time at infinite frequency	2015 April 18 04:29:05.370 UTC
Parkes beam number	4, inner ring
Beam FWHM diameter	14.1′
Beam centre (RA, dec.)	07 h 16 min 30.9 s, −19° 02′ 24.4″
Beam centre (l, b)	232.684°, −3.261°
Galaxy position (RA, dec.) ATCA epoch 1	07 h 16 min 35(3) s, −19° 00′ 40(1)″
Galaxy position (l, b) ATCA epoch 1	232.6654(1)°, −3.2348(3)°
Signal-to-noise ratio	39
Observed width, $W_{\rm obs}$	0.8 ± 0.3 ms
FRB dispersion measure	776.2(5) $\mathrm{cm^{-3}}$ pc
Dispersion index, β	−2.00(1)
Milky Way dispersion measure	188.5 $\mathrm{cm^{-3}}$ pc
Redshift, z	0.492(8)
Peak flux density, $S_{1382\,\mathrm{MHz}}$	$>2.2^{+0.6}_{-0.3}$ Jy (beam centre)
	$>2.4^{+0.5}_{-0.4}$ Jy (galaxy position)
Fluence, $\mathcal{F}_{1382\,\mathrm{MHz}}$ (Jy ms)	$1.9^{+1.1}_{-0.8}$ Jy ms (beam centre)
	$2.0^{+1.2}_{-0.8}$ Jy ms (galaxy position)
Linear polarization, L/I	$8.5 \pm 1.5\%$
Circular polarization, $\lvert V\rvert/I$	$<4.5\%$ (3σ)
Rotation measure	$36 \pm 52\,\mathrm{rad\,m^{-2}}$
Spectral index, α	$\alpha > -3.0$ (3σ, Parkes-MWA)
	$\alpha = +1.3 \pm 0.5$ (Parkes)
Comoving distance	1.88 gigaparsecs
Luminosity distance	2.81 gigaparsecs
Energy	$8^{+1}_{-5} \times 10^{38}$ ergs (galaxy position)
Luminosity	$>1.3 \times 10^{42}$ ergs $\mathrm{s^{-1}}$ (galaxy position)

The peak flux density is a band average and a lower limit due to the intrinsic width not being resolved; similarly luminosity is a lower limit. The energy quoted is the product of the band-averaged fluence, the blueshifted effective bandwidth of the observations and the square of the luminosity distance. MWA denotes the Murchison Widefield Array.

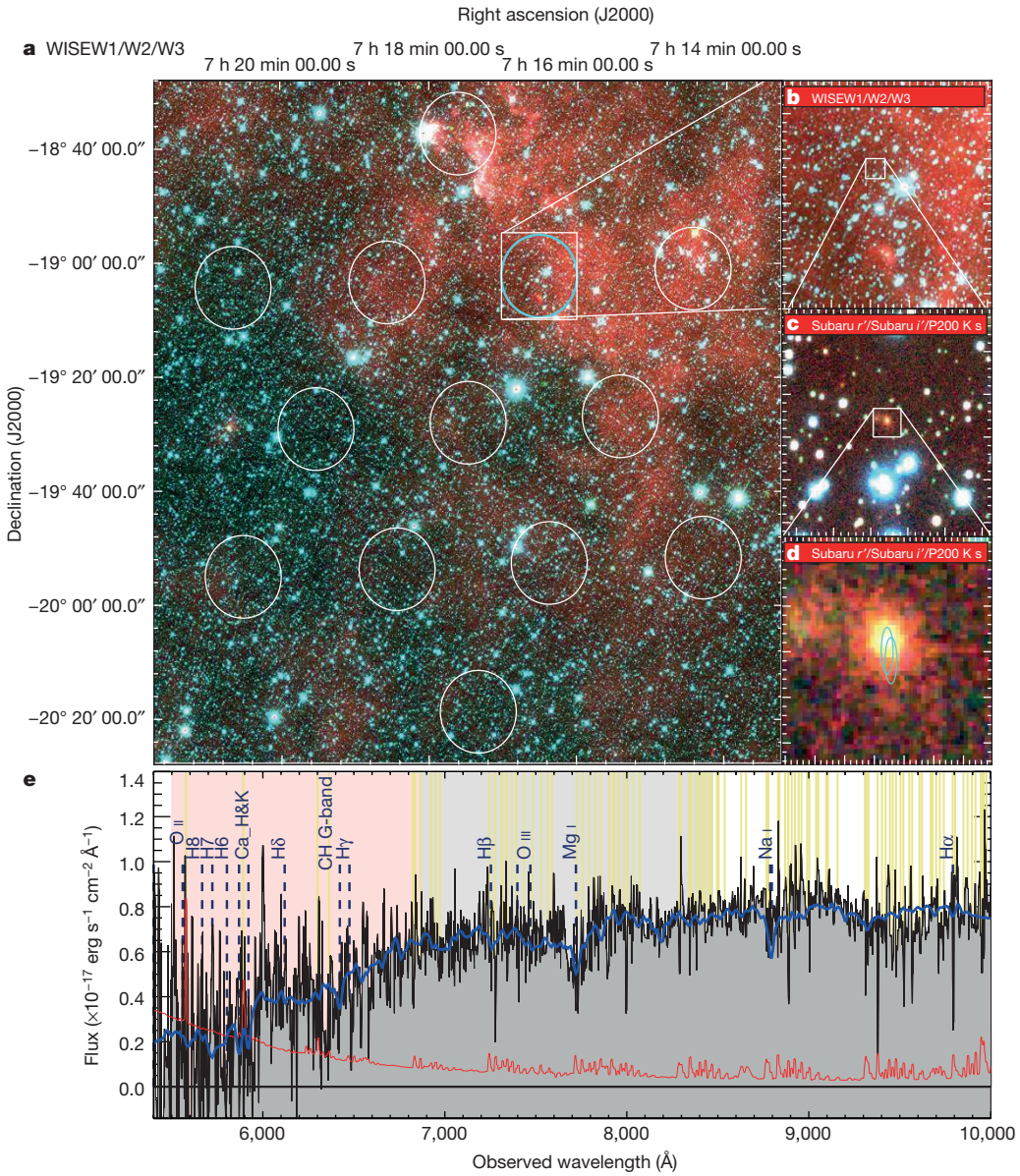

Figure 3 | Optical analysis of the FRB host galaxy. a, A wide-field composite false-colour RGB (red–green–blue) image, overplotted with the half-power beam pattern of the Parkes multi-beam receiver. Panels **b** and **c** show successive zooms on the beam 4 region, and on the fading ATCA transient location respectively. P200 K s denotes the Palomar telescope 200-inch K_s band. Panel **d** is further zoomed in with the error ellipses for the ATCA transient, as derived from both the first and second epoch, overplotted. **e**, The Subaru FOCAS spectrum de-reddened with $E(B-V)=1.2$, smoothed by five pixels and fitted to an elliptical galaxy template at $z=0.492$, denoted by the blue line. Common atomic transitions observed in galaxies are denoted by vertical dashed lines and yellow lines denote bright night sky lines. The Subaru r' and i' filter bandpasses are denoted by light red and grey background shading. The red line is the 1σ per pixel uncertainty (not smoothed).

From fitting ΛCDM cosmological models to Wilkinson Microwave Anisotropy Probe (WMAP) observations one derives[12] the cosmic density of all baryons $\Omega_{\rm baryons}=0.046\pm0.002$. Of these, about 10% are not ionized or are in stellar interiors[23] so that we expect to measure a cosmic density of ionized baryons in the intergalactic medium of $\Omega_{\rm IGM}\approx0.9\times\Omega_{\rm baryons}\approx0.041\pm0.002$. Thus, our measurement independently verifies the ΛCDM model and the WMAP observations, and constitutes a direct measurement of the ionized material associated with all of the baryonic matter in the direction of the FRB, including the so-called "missing baryons"[24]. Alternatively, if we take $\Omega_{\rm IGM}\equiv0.041$, our measurements show that $\mathrm{DM_{host}}$ is negligible.

FRB localization allows us to correct a number of observable quantities that are corrupted by the unknown gain correction factor owing to a lack of knowledge of the true position within the telescope beam. Accounting for the frequency-dependent beam response[25] we can derive a true spectral index for the FRB. We obtain $\alpha=+1.3\pm0.5$ for a fit centred at 1.382 GHz. Similarly, we derive a corrected flux density and fluence, and these, in combination with the redshift measurement, enable us to derive the distances, the energy released, the luminosity and other parameters (Table 1).

In considering the nature of the progenitor we first consider the host galaxy. An upper limit to the star-formation rate can be determined from the upper limit Hα luminosity indicated by the Subaru spectrum (see Methods) to be $\leq0.2M_{\odot}\,\mathrm{yr}^{-1}$, where $M_{\odot}$ is the solar mass. Such a low star-formation rate implies, in the simplest interpretation, that FRB models directly related to recent star formation such as magnetar flares or blitzars are disfavoured. This problem might be avoided if either some residual star formation occurred in an otherwise 'dead' galaxy, or if the FRB originated in one of the many satellite galaxies that are expected to surround an elliptical galaxy at this redshift, but that cannot be resolved in our observations. Failing these, the lack of star formation favours models such as compact merger events. This may be supported by the existence of the ~6-day radio transient, which we interpret as

the afterglow from the FRB. The presence of this short-duration radio afterglow would not be expected from models involving giant pulses from pulsars (which last only a few nanoseconds), whereas supernovae and tidal disruption events would be expected to have a longer-lasting afterglow[26]. The afterglow is consistent with the four short γ-ray bursts for which radio afterglows have been detected[27]. The stellar mass of the galaxy, derived from the optical photometry and spectroscopy (see Methods), is $\sim 10^{11} M_{\odot}$, which is in accord with the masses of elliptical host galaxies of short γ-ray bursts[28]. For a duration of 6 days for the afterglow we infer a brightness temperature of $\sim 10^{14}$ K, above the Compton cooling limit of 10^{12} K, implying a modest Doppler boosting factor. It is possible that the initial variability in brightness and spectral index is caused by scintillation, similar to that seen in the light curves of γ-ray bursts[29]. If so, this indicates a very compact initial source size.

Our conclusion that FRB 150418 is likely to be from a one-off event in an older stellar population may be at odds with the recent discovery[8] of FRB 110523. It is possible that there are two or more classes of FRB progenitor. These FRBs differ in their observed pulse widths and we speculate that this parameter might act as a discriminator between differing progenitors. FRB 150418 is not resolved (in time), but FRB 110523 appears to be (see Methods). This trend is seen in the published FRB population: some are clearly resolved, some are clearly not, although extra care needs to be taken in re-analysing this, as very slight errors in DM, as well as the effect of multi-path scattering, can make an FRB appear to have a longer intrinsic timescale.

Unresolved events like FRB 150418 might thus be ascribed to cataclysmic events (such as short γ-ray bursts), while events like FRB 110523, where the intrinsic timescale is $\sim$1 ms, could be associated to magnetar flares[30]. If so, events like FRB 150418 are unique events, whereas events like FRB 110523 could repeat, although the timescale for this is unclear. To answer these questions, and others such as whether or not some or all FRBs are standard candles, this study will need to be repeated for a large number of FRBs, and requires continued monitoring of the known FRB fields.

Online Content Methods, along with any additional Extended Data display items and Source Data, are available in the online version of the paper; references unique to these sections appear only in the online paper.

Received 27 November 2015; accepted 13 January 2016.

1. Lorimer, D. R., Bailes, M., McLaughlin, M. A., Narkevic, D. J. & Crawford, F. A bright millisecond radio burst of extragalactic origin. *Science* **318,** 777–780 (2007).
2. Keane, E. F., Stappers, B. W., Kramer, M. & Lyne, A. G. On the origin of a highly dispersed coherent radio burst. *Mon. Not. R. Astron. Soc.* **425,** L71–L75 (2012).
3. Thornton, D. *et al.* A population of fast radio bursts at cosmological distances. *Science* **341,** 53–56 (2013).
4. Spitler, L. G. *et al.* Fast radio burst discovered in the Arecibo pulsar ALFA survey. *Astrophys. J.* **790,** 101–110 (2014).
5. Burke-Spolaor, S. & Bannister, K. W. The galactic position dependence of fast radio bursts and the discovery of FRB 011025. *Astrophys. J.* **792,** 19–26 (2014).
6. Ravi, V., Shannon, R. M. & Jameson, A. A fast radio burst in the direction of the Carina dwarf spheroidal galaxy. *Astrophys. J.* **799,** L5–L10 (2015).
7. Petroff, E. *et al.* A real-time fast radio burst: polarization detection and multiwavelength follow-up. *Mon. Not. R. Astron. Soc.* **447,** 246–255 (2015).
8. Masui, K. *et al.* Dense magnetized plasma associated with a fast radio burst. *Nature* **528,** 523–525 (2015).
9. Champion, D. *et al.* Five new fast radio bursts from the HTRU high latitude survey: RST evidence for two-component bursts. *Mon. Not. R. Astron. Soc.* (submitted); preprint at http://arxiv.org/abs/1511.07746 (2015).
10. McQuinn, M. Locating the "missing" baryons with extragalactic dispersion measure estimates. *Astrophys. J.* **780,** L33 (2014).
11. Zhou, B., Li, X., Wang, T., Fan, Y.-Z. & Wei, D.-M. Fast radio bursts as a cosmic probe? *Phys. Rev. D* **89,** 107303 (2014).
12. Hinshaw, G. *et al.* Nine-year Wilkinson Microwave Anisotropy Probe (WMAP) observations: cosmological parameter results. *Astrophys. J.* **208** (Suppl.), 19 (2013).
13. Chandra, P. & Frail, D. A. A. Radio-selected sample of gamma-ray burst afterglows. *Astrophys. J.* **746,** 156 (2012).
14. Cordes, J. M. & Lazio, T. J. W. NE2001.I. A new model for the Galactic distribution of free electrons and its fluctuations. Preprint at http://arxiv.org/abs/astro-ph/0207156 (2002).
15. Bhat, N. D. R., Cordes, J. M., Camilo, F., Nice, D. J. & Lorimer, D. R. Multifrequency observations of radio pulse broadening and constraints on interstellar electron density microstructure. *Astrophys. J.* **605,** 759–783 (2004).
16. Bell, M. E. *et al.* A search for variable and transient radio sources in the extended Chandra Deep Field South at 5.5 GHz. *Mon. Not. R. Astron. Soc.* **450,** 4221–4232 (2015).
17. Brown, M. J. I., Jannuzi, B. T., Floyd, D. J. E. & Mould, J. R. The ubiquitous radio continuum emission from the most massive early-type galaxies. *Astrophys. J.* **731,** L41 (2011).
18. Mooley, K. P. *et al.* The Caltech-NRAO Stripe 82 Survey (CNSS) paper I: the pilot radio transient survey in 50 deg^2. *Astrophys. J.* (in the press); http://arxiv.org/abs/1601.01693 (2016).
19. Ioka, K. The cosmic dispersion measure from gamma-ray burst afterglows: probing the reionization history and the burst environment. *Astrophys. J.* **598,** L79–L82 (2003).
20. Inoue, S. Probing the cosmic reionization history and local environment of gamma-ray bursts through radio dispersion. *Mon. Not. R. Astron. Soc.* **348,** 999–1008 (2004).
21. Dolag, K., Gaensler, B. M., Beck, A. M. & Beck, M. C. Constraints on the distribution and energetics of fast radio bursts using cosmological hydrodynamic simulations. *Mon. Not. R. Astron. Soc.* **451,** 4277–4289 (2015).
22. Xu, J. & Han, J. L. Extragalactic dispersion measures of fast radio bursts. *Res. Astron. Astrophys.* **15,** 1629 (2015).
23. Fukugita, M. & Peebles, P. J. E. The cosmic energy inventory. *Astrophys. J.* **616,** 643–668 (2004).
24. Bregman, J. N. The search for the missing baryons at low redshift. *Annu. Rev. Astron. Astrophys.* **45,** 221–259 (2007).
25. Staveley-Smith, L. *et al.* The Parkes 21 cm multibeam receiver. *Publ. Astron. Soc. Aust.* **13,** 243–248 (1996).
26. Pietka, M., Fender, R. P. & Keane, E. F. The variability time-scales and brightness temperatures of radio flares from stars to supermassive black holes. *Mon. Not. R. Astron. Soc.* **446,** 3687–3696 (2015).
27. Fong, W., Berger, E., Margutti, R. & Ashley, B. A. A decade of short-duration gamma-ray burst broad-band afterglows: energetics, circumburst densities, and jet opening angles. *Astrophys. J.* **815,** 102 (2015).
28. Berger, E. Short-duration gamma-ray bursts. *Annu. Rev. Astron. Astrophys.* **52,** 43–105 (2014).
29. Frail, D. A., Kulkarni, S. R., Nicastro, L., Feroci, M. & Taylor, G. B. The radio afterglow from the γ-ray burst of 8 May 1997. *Nature* **389,** 261–263 (1997).
30. Kulkarni, S. R., Ofek, E. O. & Neill, J. D. The Arecibo fast radio burst: dense circum-burst medium. Preprint at http://arxiv.org/abs/1511.09137 (2015).

Acknowledgements The Parkes radio telescope and the Australia Telescope Compact Array are part of the Australia Telescope National Facility, which is funded by the Commonwealth of Australia for operation as a National Facility managed by CSIRO. Parts of this research were conducted by the Australian Research Council Centre of Excellence for All-sky Astrophysics (CAASTRO) and used the gSTAR national facility at Swinburne University of Technology. Parts of this work are based on data collected at the Subaru Telescope, which is operated by the National Astronomical Observatory of Japan, the Murchison Radio-astronomy Observatory operated by CSIRO, the Giant Metrewave Radio Telescope (GMRT), which is run by the National Centre for Radio Astrophysics of the Tata Institute of Fundamental Research, the Sardinia Radio Telescope as part of scientific commissioning of the telescope, and the 100-m telescope of the MPIfR at Effelsberg. We acknowledge the Wajarri Yamatji people as the traditional owners of the MWA Observatory site.

Author Contributions E.F.K. is the principal investigator of the SUPERB project, created SUPERB survey infrastructure at Parkes and Swinburne, led survey planning, formulated and wrote (with input from co-authors) the contents of this manuscript, performed the Ω_{IGM} calculation, calculated the FRB spectral index, produced the FRB waterfall plot and the light curve plot. S.J. and S.B. performed ATCA observations and data analysis. S.J. and B.W.S. worked on radio light curve interpretation. S.B., N.D.R.B. and P.C. performed GMRT observations and data analysis. E.B. created survey infrastructure at Parkes and Swinburne and created the MWA shadowing infrastructure. Additionally, E.F.K., S.J., S.B., E.B., N.D.R.B., M. Burgay, M.C., C.F., M.K., E.P., A.P., W.v.S., M. Bailes., S.B.-S. and R.P.E. all performed observations for the SUPERB survey at Parkes. A.J. created and maintained the Parkes and Swinburne hardware and software infrastructure and performed data management for the SUPERB project. M. Bailes additionally provided Parkes and Swinburne hardware. C.F. and M.K. also worked on the calculation of the cosmic density of ionized baryons in the intergalactic medium. M.K. additionally performed FRB radio profile fitting. Polarization analysis of the FRB signal was performed by M.C., E.P. and W.v.S. W.v.S. also produced the polarization profile plot. E.P. additionally performed the Swift analysis. Non-imaging radio follow-up was performed by M. Burgay, A.P. and D.P. with the Sardinia Radio Telescope, by R.P.E. and M. Berezina with the Effelsberg Radio Telescope, and by B.W.S., M.M. and C.B. at the Lovell Telescope at Jodrell Bank. T. Totani, M.H., H.F., T.H., T.M., Y.N., H.S., T. Terai, N.T, S.Y. and N.Y. performed the Subaru observations. T. Totani, T.H., N.T. and S.Y. additionally performed Subaru data analysis, determined the spectral redshift and created the optical profile plot. C.F., T. Totani, S.Y. and R.A. performed the optical profile fitting. J.C. performed data analysis on the Keck and Subaru data, also obtained the spectral redshift and produced the optical spectrum plot. J.J. performed the Palomar observations. M.M.K. performed the Keck observation. MWA observations were performed by N.D.R.B., D.L.K., S.J.T., A.W. and R.W. with data analysis by D.L.K. and S.J.T. D.L.K. additionally measured the photometric redshift and produced the RGB (red–green–blue) image and photo-z plots (Extended Data Fig. 1).

Author Information Reprints and permissions information is available at www.nature.com/reprints. The authors declare no competing financial interests. Readers are welcome to comment on the online version of the paper. Correspondence and requests for materials should be addressed to E.F.K. (e.keane@skatelescope.org).

METHODS

DM contributions. When radio signals propagate through a plasma, the travel time is longer than the light travel time in a vacuum. The additional delay depends on the radio wave frequency, f, in units of GHz, and obeys a precise physical law of the form: $t_{DM} = 4.149\,\mathrm{ms} \times (\mathrm{DM} \times f^{-2})$, where the DM is the integrated electron density along the line of sight in units of $\mathrm{cm}^{-3}\,\mathrm{pc}$. If travelling across cosmological distances there are several contributions to the observed DM—from the host, the intergalactic medium and the Milky Way. The quantity of interest is the intergalactic medium component because this can be used, in conjunction with redshift measurements, to perform a number of fundamental studies, for example, detecting the missing baryons[10], determining the dark energy equation of state[11] and, if the signal is linearly polarized, measuring magnetic field strengths in the intergalactic medium[31]. For these applications the DM contributions other than those from the intergalactic medium are essentially foregrounds which must be understood so that they can be removed. Here we examine each contribution in turn and note the uncertainties in each case; it is important to note that the precision in the observed DM value is high (see Table 1) and does not therefore contribute to the uncertainty in determining the DM for the intergalactic medium.

The Milky Way component consists of two parts, the first of which is that due to the interstellar medium. This is in principle known[14], because the NE2001 model of the Galaxy's electron density can determine this to an accuracy of approximately 20%. The second Milky Way component is the contribution from the dark matter halo, which is thought to exist, yet which is not included in the NE2001 model. We follow previous work[21], which has calculated this term to be $30\,\mathrm{cm}^{-3}\,\mathrm{pc}$. It is unclear how to assign an uncertainty to this component so (considering that the other components are dominant regardless) we take it to be zero. The host component is suppressed by a factor of $(1+z)^1$. Its magnitude depends on both the nature of the progenitor and of the host galaxy.

The observed FRB signal can be used to constrain the progenitor's local DM contribution—a non-negligible contribution could imply a high density of electrons to be located close to the source. Such a high density configuration[32] could produce higher-order dispersion terms (that is, the pulse's frequency dispersion would deviate from the quadratic form), could result in plasma frequencies comparable to the emitted frequency (that is, radiation would not escape), and could produce scattering in the pulse profile. None of these effects are observed for FRB 150418, implying that any local-progenitor DM component is negligible.

The host galaxy contribution has been examined recently[22] for spiral, dwarf and elliptical galaxies. This work considered modified versions of NE2001, with various sub-components of the model included or excluded as appropriate and suitable scalings to the Hα luminosity applied. For an elliptical galaxy, which is relevant in the case of FRB 150418, the average DM contribution over all inclination angles is $37\ \mathrm{cm}^{-3}\,\mathrm{pc}$ (this is the value before being suppressed by the $(1+z)^1$ factor) and we use this as our estimate of the host contribution. As this is based upon NE2001 we assume that a 20% uncertainty applies. In addition to the uncertainties mentioned already the intergalactic medium component itself is uncertain at the level of $\sim 100\,\mathrm{cm}^{-3}\,\mathrm{pc}$, owing to inhomogeneities between different lines of sight through the intergalactic medium[10].

SUPERB. SUPERB is a project ongoing at the 64-m Parkes radio telescope since April 2014 with goals of discovering FRBs and pulsars. The central frequency of the survey is 1.382 GHz, with a bandwidth of 400 MHz, of which about 340 MHz is typically usable. It uses optimized graphics processing unit codes for performing real-time radio frequency interference mitigation and searches for short-duration radio bursts and pulsars in relativistic binary systems. In the real-time search we use the following criteria to define candidate FRB events: (1) the DM of the burst must be at least 1.5 times the expected maximum Milky Way contribution; (2) the signal-to-noise ratio must be at least 10; (3) the signal cannot be detected in more than four beams of the 13-beam receiver used for the SUPERB project at Parkes—an event detected in more beams cannot originate from a boresight signal and therefore cannot be of a celestial origin; (4) the width must be less than or equal to 8.192 ms, that is, 128 times our native time sampling of 64 μs; and (5) the number of independent events detected in a 4-s window centred on the event in question must be no greater than 5. The lag between the FRB signal hitting the dish and our software informing us of the detection[7] is only ~10 s. We further search the data, offline, with more stringent interference rejection and covering corners of parameter space ignored for expediency during the real-time search. We note that since instigating this search system at Parkes no FRB has been missed by the real-time search pipeline, including FRB 150418.

FRB 150418 was detected in beam 4 of the 21-cm multi-beam receiver. The FRB profile was fitted simultaneously for time of arrival, DM, width, amplitude and dispersion index using 4 and 8 different sub-bands. The results were consistent with an unresolved pulse, where the width is purely given by the dispersion smearing across the 390.625-kHz filterbank channels. Uncertainties were determined using CERN's MINUIT packages (http://seal.web.cern.ch/seal/snapshot/work-packages/mathlibs/minuit/). The burst was found to have a DM of 776.2(5) $\mathrm{cm}^{-3}\,\mathrm{pc}$, and a dispersion index of $\beta = -2.00(1)$, where the dispersion delay is proportional to ν^{β}, and so is consistent with propagation through a cold plasma.

The gain of beam 4 is well fitted by a Gaussian[25] with FWHM of 14.1 arcmin, so to derive corrected values for the flux density, fluence, and so on we boost the measured values by a factor of $\exp(\ln 2(2\theta/\mathrm{FWHM})^2)$, where θ is the offset of the signal from the beam centre. The offset between the ATCA position determined from the first epoch (RA 07 h 16 min 34.557 s, dec. −19° 00′ 39.954″) and the centre of the Parkes beam (RA 07 h 16 min 30.9 s, dec. −19° 02′ 24.4″) is $\theta = 1.944$ arcmin, yielding a boost factor of 1.054. The observed peak flux density, if the FRB were at the centre of the beam, is 2.2 Jy with a corresponding fluence of 1.9 Jy ms; correcting these to the location of the host galaxy, we estimate values of 2.4 Jy and 2.0 Jy ms.

A calibration observation was taken 17 min post-burst and the polarization calibration was performed using the PSRCHIVE software package[33]. On the basis of observations of PSR J1644–4459, a bright polarized pulsar which we use to calibrate the off-axis response, taken three days before the FRB, we determine that the difference in the Jones matrix coefficients is not statistically different off-boresight. Therefore the boresight calibration was used to determine the polarization fraction of the pulse. This FRB is not seen to have a large linear polarization L, the rotation-measure-corrected linear polarization is $L/I = 8.5 \pm 1.5\%$ (where I is total intensity) and the circular polarization is consistent with zero. An additional systematic uncertainty exists in the leakage of total intensity to polarization. Our analysis of PSR J1644–4459 provides an upper limit on the magnitude (but not orientation) of the leakage vector that is <6% of the total intensity, meaning that the true L/I value may be either smaller or larger than quoted by up to this amount. Owing to the low linear polarization the rotation measure estimate is not very precise at $36 \pm 52\ \mathrm{rad\,m}^{-2}$. As the rotation measure is consistent with zero, examination of the intergalactic medium magnetic field strength is not possible with this FRB, although for completeness we note that the 3σ upper limit on the electron weighted intergalactic medium magnetic field strength is ~0.4 μG for this line of sight. There is no evidence for a large host contribution to the rotation measure for this FRB, although we note that an extremely large rotation measure exceeding $10^5\ \mathrm{rad\,m}^{-2}$ would result in depolarization within a single frequency channel, meaning we are insensitive to such large values.

The Murchison Widefield Array (MWA)[34] was shadowing our Parkes observations but did not detect a counterpart. The resulting 3σ fluence upper limit of 1,050 Jy ms at 185 MHz gives us the first simultaneous multi-frequency observation of an FRB, and hence the first broadband limit on the spectral index. The spectral index limit from the Parkes and MWA data combined is $\alpha > -3.0$. Properties of the FRB are summarized in Table 1.

Follow-up observations. After the discovery of the FRB we triggered observations at numerous telescopes and performed a calibration observation at Parkes. We continued to observe with the Parkes telescope, obtaining 4.5 h of observation over the course of the next 7.5 h, in order to search for any repeat bursts. The MWA was shadowing during the discovery observation and continued to track the FRB position for another ~7.5 h. The ATCA was on source 2 h after the burst and also observed until $T + 7.5$ h (where T is the time of the FRB) when the source set at both Parkes and ATCA. Swift was on source 8 h after the burst, and 10 h after the burst the Lovell telescope continued the monitoring for 2.5 h. On April 19 and 20 we obtained optical observations with Subaru, and on April 20 and 21 continued to search for repeated radio bursts with the Effelsberg, Sardinia and Parkes radio telescopes. The longer term follow-up campaign consisted of radio imaging (four further ATCA epochs, three GMRT epochs), high time resolution radio (with the Lovell telescope), X-ray (one further Swift epoch), optical photometry (with the Palomar telescope) and optical spectroscopy (with the Keck and Subaru telescopes). We did not detect any subsequent bursts in our high time resolution radio follow-up (limiting flux densities in Extended Data Table 1); however, regular emission at a much weaker level cannot be ruled out. The follow-up observations are summarized in Extended Data Table 1. We additionally note that no γ-ray burst was detected in temporal coincidence, or in the months before, by telescopes on either of the Fermi or Swift satellites. Furthermore, at a comoving distance of 1.8 gigaparsecs or a luminosity distance of 2.8 gigaparsecs, this galaxy is beyond the LIGO[35] horizon for gravitational wave signatures from short γ-ray bursts.

Imaging transients. The radio transient sky is not very well studied at frequencies of 5.5 GHz and 7.5 GHz to the flux density levels relevant to this study. Additionally there are no archival data of the FRB field with which to compare our follow-up observations. To estimate the likelihood of the 6-day fading transient being detected by chance in our ATCA follow-up of the Parkes FRB field we first considered a previous ATCA study[16]. This is the only such work performed on the same timescales and at the same observing frequency using the ATCA. In that work, which also covered a wider area of sky than our FRB follow-ups and to a

deeper level, no transient sources were discovered. A 95% (99%) confidence upper limit event rate of <7.5 deg^{-2} (<11.1 deg^{-2}) with a flux density of $>69\,\mu$Jy/beam was obtained. Scaling this to obtain the expectation of a transient with flux density in excess of 200 μJy yields an upper limit event rate of <1.5 deg^{-2} (<2.2 deg^{-2}). Considering the 0.04-deg^2 field-of-view of a Parkes beam, which corresponds to the uncertainty in the FRB's position, the upper limit on the expected number of events in our follow-up observations is thus <0.06 (<0.09). We can rephrase this by interpreting the upper limit number of expected events as the upper limit on λ, the Poisson rate parameter; then the probability of a chance temporal coincidence is $P(1;\lambda)=\lambda\exp(-\lambda)$. This yields an upper-limit probability of $<6\%$ ($<8\%$).

One can also obtain estimates of the false-positive rate from considering studies[36–40] at other telescopes. As other studies are not ideally matched in terms of observing frequency and sensitivity, one must scale the findings appropriately. For example, for studies performed at different observing frequencies we must scale the flux densities by a spectral index; we adopt the spectral index of our 6-day transient as measured in the first epoch of our follow-up. Additionally, sensitivity levels must be scaled to the 200-μJy level; for this operation we adopt the standard $N\propto S^{-3/2}$ scaling. With this approach we consider a recent deep Very Large Array study[18] which operated at 2–4 GHz. Applying the appropriate scaling, this study yields an expected number of events in our follow-up observations of <0.001 (<0.002) at 95% (99%) confidence. The equivalent upper limit chance temporal coincidence probability is $<0.1\%$ ($<0.2\%$). This result is more constraining than the ATCA-derived numbers by a factor of at least 60. From this assessment we deem it statistically unlikely that we would have detected, by chance, this fading negative spectral index radio source at this location and time, resulting in our interpretation that this source is likely to be associated with the FRB.

Ideally, we might expand upon this calculation by estimating probabilities of chance coincidence in each independent wave-band (radio, optical and X-ray) in our follow-up campaign, and then compute a joint probability of a transient occurring in any of the bands. It is unclear what the appropriate statistics are for the X-ray and optical bands, but if we take the observed γ-ray burst and supernova rates as indicative, we find that the upper limit expectation in these wave bands is much smaller than in the radio bands. Deeper all-sky radio transient surveys are therefore the key to tightening constraints on transient associations like that reported here.

Optical analysis. The i' optical profile of the Galaxy was fitted with a Sersic function of the form $I(r)\propto\exp(-kR^{1/n})$. The best-fit parameters (see Extended Data Fig. 2) are a Sersic index of $n=3.6\pm0.5$, consistent with the $n=4$ value seen in elliptical galaxies. The half-light radius is $R_e=6.9\pm1.2$ pixels, or $R_e=1.4\pm0.2$ arcsec. At $z=0.492$ the angular diameter distance is 1.62 gigaparsecs so that this implies $R_e=10.9\pm1.8$ kpc as the physical half-light radius of the galaxy. The profile fitting also yields an estimate of the major to minor axes ratio for the galaxy of $b/a=0.68\pm0.03$. We note that there are additional systematic uncertainties involved in the fit of the Sersic index, depending on the exact method of sky subtraction employed; our analysis suggests that the systematic errors are probably of equal magnitude to the statistical errors quoted above.

We obtained the following photometry of the FRB host galaxy: with Subaru Suprime-Cam[41] we determined AB magnitudes of 23.45(16) and 22.07(31), for the r' and i' bands respectively. Between the two Subaru epochs no variability is seen—a subtraction of the epochs yields an upper limit on any variation of 25.2 and 24.7 magnitudes (5σ). The galaxy is also detected in two WISE filters with Vega magnitudes of 15.204(0.044) and 15.050(082), for the W_1 and W_2 bands respectively. With the Palomar 200″ (P200) telescope we obtained further information, obtaining Vega magnitudes of 18.92(10), 17.55(25) and 16.51(05) for the J, H and K_s bands respectively. We corrected the observed photometry for the Milky Way extinction using $A_V=3.7$ mag and standard extinction coefficients[42], and converted those magnitudes into flux densities using the established zero-points[43,44]. We fitted for the photometric redshift using the 2015 November version of EAZY[45], finding 68% confidence limits for $0.48<z<0.56$. This was robust to different choices of galaxy template, with good overall fits (χ^2 of 5–8). We then fitted the spectral energy distribution of the host galaxy using MAGPHYS[46]. We were able to achieve an acceptable fit (see Extended Data Fig. 1) to all of the photometry with a model for a passive ($\leq0.2M_\odot\,\mathrm{yr}^{-1}$), massive (stellar mass $\sim10^{11}M_\odot$) galaxy with a modest amount of dust (in-host extinction A_V in the range 0–4 mag). The exact fit was rather degenerate because of our limited wavelength coverage, with only the stellar mass well determined. Future observations at shorter wavelengths should be able to determine more robust properties.

The spectrum that confirmed the redshift was obtained on 2015 November 2 in a 3-h observation using FOCAS on the Subaru telescope. An earlier attempt to obtain a spectroscopic redshift on 2015 October 21 using DEIMOS on the Keck telescope in poorer sky conditions had proved difficult to calibrate and resulted in an imprecise redshift estimate, no better than the photometric estimate. In that case difficulties in calibration are compounded by the spectrum's lack of any relevant emission lines. The well calibrated Subaru spectrum is found to be consistent with a reddened $z=0.492(8)$ early-type galaxy with $E(B-V)=1.2\pm0.1$ (Fig. 3), noting that r' and i' are approximations to restframe B and V filters. This implies absolute magnitudes of $M_B\approx-21.6$ and $M_V\approx-22.1$. As the galaxy is elliptical we can apply the Faber–Jackson relation[47] to estimate the velocity dispersion of $\sim230\,\mathrm{km\,s}^{-1}$. From the virial theorem and the observed half-light radius we can thus estimate the stellar (and total) mass[48] to be $\sim10^{11}M_\odot$ (and $\sim2\times10^{12}M_\odot$). An upper limit to the Hα luminosity of $2.6\times10^{40}\,\mathrm{erg\,s}^{-1}$ (3σ) can be derived from the optical spectrum, and from this we can, in the standard way[49], derive a star-formation rate of $\leq0.2M_\odot\,\mathrm{yr}^{-1}$.

The very faint companion galaxy ($r'=24.22(16)$ mag, $i'=23.22(31)$ mag) visible to the northeast is not inconsistent with a galaxy at the same redshift. If confirmed the two galaxies may be in the process of merging. The absolute K-band magnitude of the galaxy is -25.7 mag (Vega). The radio continuum level can be estimated from this[17] and is consistent with the quiescent level of the galaxy after the ∼6-day fading event. This shows that the background level seen is not surprising for an early-type galaxy, and implies that the FRB afterglow had already faded below this level by the third ATCA epoch.

FRB 110523. After the initial submission of this manuscript a study was published[8] announcing the discovery of FRB 110523, which we have compared and contrasted with FRB 150418 in the main text. There are now strong indications that there are two or more FRB progenitors, and we speculate that the observed pulse width may act as a useful discriminator between these. To this end we consider the time sampling and frequency resolution of the study that discovered FRB 110523, as well as its DM, in an effort to see whether the pulse was resolved in the Green Bank observations[8]. We would expect an unresolved FRB to have an observed width of no more than 1.08 ms, 1.14 ms and 1.26 ms in the highest, central and lowest frequency channels, respectively, in the Green Bank study[8]. This is inconsistent with the reported observed width (after the effects of scattering had been removed) at the 3σ to 4σ level, indicating that FRB 110523 appears to be resolved and therefore to have an intrinsic timescale of ∼1 ms.

31. Zheng, Z., Ofek, E. O., Kulkarni, S. R., Neill, J. D. & Juric, M. Probing the intergalactic medium with fast radio bursts. *Astrophys. J.* **797,** 71 (2014).
32. Dennison, B. Fast radio bursts: constraints on the dispersing medium. *Mon. Not. R. Astron. Soc.* **443,** L11–L14 (2014).
33. Hotan, A. W., van Straten, W. & Manchester, R. N. PSRCHIVE and PSRFITS: an open approach to radio pulsar data storage and analysis. *Publ. Astron. Soc. Aust.* **21,** 302–309 (2004).
34. Tingay, S. J. *et al.* The Murchison Widefield Array: The Square Kilometre Array precursor at low radio frequencies. *Publ. Astron. Soc. Aust.* **30,** e007 (2013).
35. Abbott, B. P. *et al.* LIGO: the Laser Interferometer Gravitational-Wave Observatory. *Rep. Prog. Phys.* **72,** 076901 (2009).
36. Becker, R. H., Helfand, D. J., White, R. L. & Proctor, D. D. Variable radio sources in the Galactic Plane. *Astron. J.* **140,** 157–166 (2010).
37. Ofek, E. O. *et al.* A very large array search for 5 GHz radio transients and variables at low galactic latitudes. *Astrophys. J.* **740,** 65 (2011).
38. Frail, D. A., Kulkarni, S. R., Ofek, E. O., Bower, G. C. & Nakar, E. A revised view of the transient radio sky. *Astrophys. J.* **747,** 70 (2012).
39. Croft, S., Bower, G. C. & Whysong, D. The Allen Telescope Array Pi GHz Sky Survey. III. The ELAIS-N1, Coma, and Lockman hole fields. *Astrophys. J.* **762,** 93 (2013).
40. Gal-Yam, A. *et al.* Radio and optical follow-up observations of a uniform radio transient search: implications for gamma-ray bursts and supernovae. *Astrophys. J.* **639,** 331–339 (2006).
41. Miyazaki, S. *et al.* Subaru Prime Focus Camera—Suprime-Cam. *Publ. Astron. Soc. Jpn* **54,** 833–853 (2002).
42. Davenport, J. R. A. *et al.* The SDSS-2MASS-WISE 10-dimensional stellar colour locus. *Mon. Not. R. Astron. Soc.* **440,** 3430–3438 (2014).
43. Cohen, M., Wheaton, W. A. & Megeath, S. T. Spectral irradiance calibration in the infrared. XIV. The absolute calibration of 2MASS. *Astron. J.* **126,** 1090–1096 (2003).
44. Jarrett, T. H. *et al.* The Spitzer-WISE survey of the ecliptic poles. *Astrophys. J.* **735,** 112 (2011).
45. Brammer, G. B., van Dokkum, P. G. & Coppi, P. EAZY: a fast, public photometric redshift code. *Astrophys. J.* **686,** 1503–1513 (2008).
46. da Cunha, E., Charlot, S. & Elbaz, D. A simple model to interpret the ultraviolet, optical and infrared emission from galaxies. *Mon. Not. R. Astron. Soc.* **388,** 1595–1617 (2008).
47. Faber, S. M. & Jackson, R. E. Velocity dispersions and mass-to-light ratios for elliptical galaxies. *Astrophys. J.* **204,** 668–683 (1976).
48. Bullock, J. S. *et al.* Profiles of dark haloes: evolution, scatter and environment. *Mon. Not. R. Astron. Soc.* **321,** 559–575 (2001).
49. Kennicutt, R. C. Jr. The global Schmidt law in star-forming galaxies. *Astrophys. J.* **498,** 541–552 (1998).

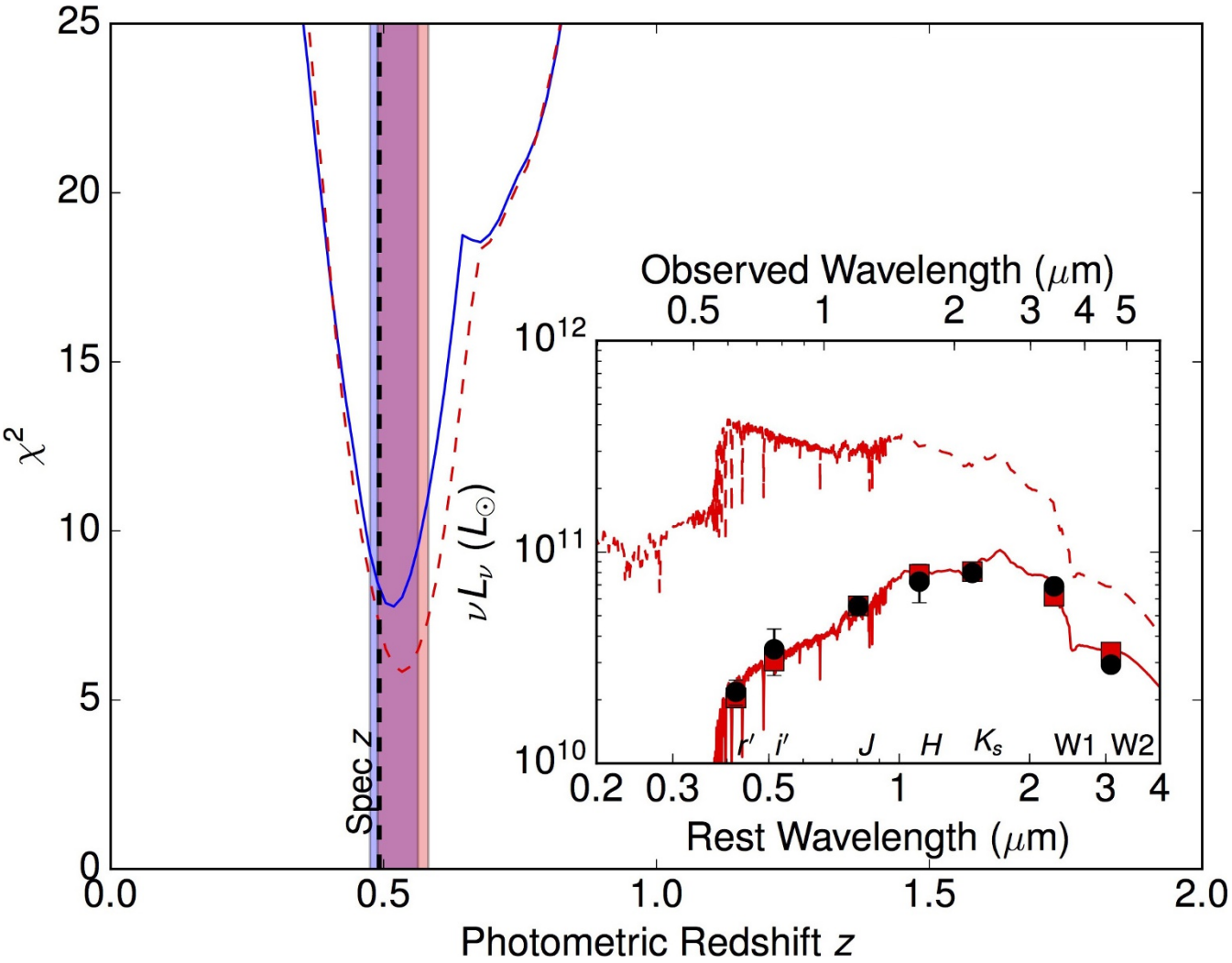

Extended Data Figure 1 | The photometric redshift of the FRB host galaxy. A χ^2 fit of the redshift of the galaxy based on the spectral energy (L_ν) distribution is shown. The photometric redshift determined from this is $0.48 < z < 0.56$ (68% confidence, denoted by the shaded regions). Two spectral fits are shown, and these are denoted by the red and blue shading respectively. The spectral redshift is denoted by the dashed vertical line. The inset shows the spectral energy distribution fit, with the seven photometric estimates overplotted with 1σ error bars.

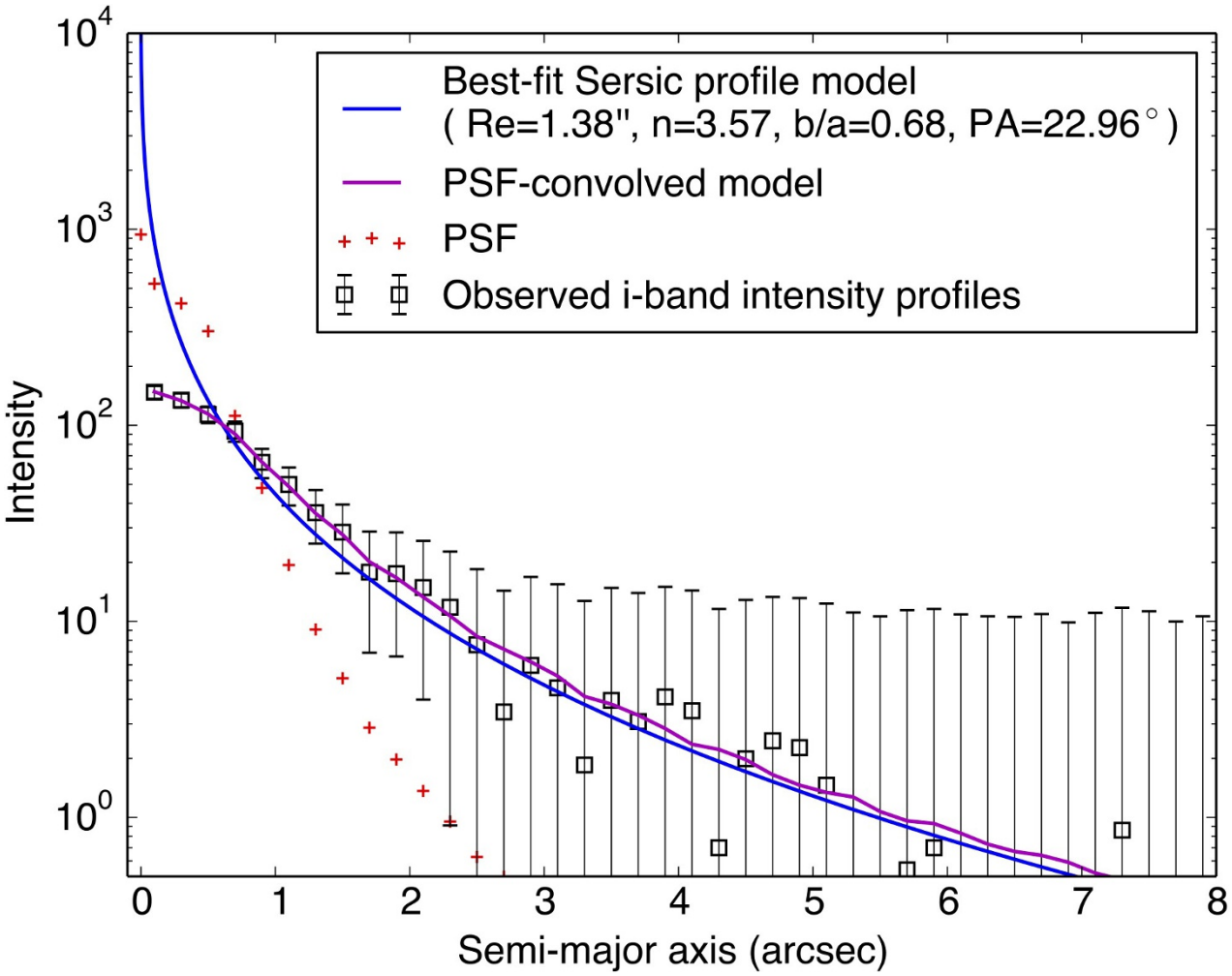

Extended Data Figure 2 | The optical surface brightness profile of the FRB host galaxy. The surface brightness profile of the galaxy in the Subaru i' band image was fitted to an ellipsoidal Sersic function. Best-fit values for the half-light radius (R_e), Sersic index (n), axis ratio (b/a) and position angle (PA) are given in the inset. The model profiles and data are shown as the flux along an ellipse as a function of semi-major axis. The image point spread function (PSF) profile is also shown as a function of radius. Error bars give the root-mean-square scatter of the pixel counts along the axis.

Extended Data Table 1 | Summary of follow-up observations of FRB 150418

Time (UTC)	Telescope	Band	Tobs (s)	Mode	Level/limit
2015-04-18-04:21:15	Parkes	1.4 GHz	561	TD*	2.2 Jy
Shadowing	MWA	185 MHz	27000	TD	< 1050 Jy ms
2015-04-18-04:31:08	Parkes	1.4 GHz	465	TD	$< 0.17(W/0.9\ \mathrm{ms})^{-0.5}$ Jy
2015-04-18-05:04:35	Parkes	1.4 GHz	1181	TD	$< 0.17(W/0.9\ \mathrm{ms})^{-0.5}$ Jy
2015-04-18-06:30:15	ATCA	5.5,7.5 GHz	19800	RI*	$0.27(5)$ mJy/beam, $0.18(3)$ mJy/beam
2015-04-18-07:46:27	Parkes	1.4 GHz	3618	TD	$< 0.17(W/0.9\ \mathrm{ms})^{-0.5}$ Jy
2015-04-18-08:47:28	Parkes	1.4 GHz	3618	TD	$< 0.17(W/0.9\ \mathrm{ms})^{-0.5}$ Jy
2015-04-18-09:48:09	Parkes	1.4 GHz	3617	TD	$< 0.17(W/0.9\ \mathrm{ms})^{-0.5}$ Jy
2015-04-18-10:48:59	Parkes	1.4 GHz	3617	TD	$< 0.17(W/0.9\ \mathrm{ms})^{-0.5}$ Jy
2015-04-18-11:49:37	Parkes	1.4 GHz	758	TD	$< 0.17(W/0.9\ \mathrm{ms})^{-0.5}$ Jy
2015-04-18-12:20:57	*Swift*	X-ray	3976	PC	$< 7.1 \times 10^{-14}$ erg/cm^2/s
2015-04-18-14:22:52	Lovell	1.4 GHz	7200	TD	$< 0.11(W/0.9\ \mathrm{ms})^{-0.5}$ Jy
2015-04-19-06:06:19	Subaru	i'	600	Ph*	22.06(31) mag (AB)
2015-04-19-06:37:12	Subaru	r'	900	Ph*	23.33(16) mag (AB)
2015-04-20-05:50:27	Subaru	i'	1200	Ph*	22.08(31) mag (AB)
2015-04-20-06:30:53	Subaru	r'	1200	Ph*	23.59(16) mag (AB)
2015-04-20-15:49:09	Effelsberg	1.4 GHz	8300	TD	$< 0.11(W/0.9\ \mathrm{ms})^{-0.5}$ Jy
2015-04-21-06:40:42	Parkes	1.4 GHz	3600	TD	$< 0.17(W/0.9\ \mathrm{ms})^{-0.5}$ Jy
2015-04-21-17:21:40	SRT	1.4 GHz	3600	TD	$< 0.61(W/0.9\ \mathrm{ms})^{-0.5}$ Jy
2015-04-24-02:44:15	ATCA	5.5,7.5 GHz	72900	RI*	$0.23(2)$ mJy/beam, < 0.08 mJy/beam
2015-04-26-01:45:05	ATCA	5.5,7.5 GHz	74700	RI*	$0.09(2)$ mJy/beam, < 0.08 mJy/beam
2015-05-07-03:18:42	*Swift*	X-ray	2908	PC	$< 9.3 \times 10^{-14}$ erg/cm^2/s
2015-05-18-12:30:00	GMRT	0.61 GHz	7200	RI	< 0.35 mJy/beam
2015-05-22-12:42:00	GMRT	1.4 GHz	7140	RI	< 0.15 mJy/beam
2015-06-04-21:12:15	ATCA	5.5,7.5 GHz	26700	RI*	$0.11(2)$ mJy/beam, < 0.09 mJy/beam
2015-10-15-05:32:23	Lovell	1.4 GHz	7200	TD	$< 0.14(W/0.9\ \mathrm{ms})^{1/2}$ Jy ms
2015-10-21-00:14:15	Keck	OIR	3600	Sp*	see Subaru observation
2015-10-27-14:09:35	ATCA	5.5,7.5 GHz	30600	RI*	$0.09(2)$ mJy/beam, < 0.07 mJy/beam
2015-10-31-11:15:54	P200	J	1080	Ph*	18.92(10) mag (Vega)
2015-10-31-11:38:31	P200	H	450	Ph*	17.55(25) mag (Vega)
2015-10-31-11:51:15	P200	K_s	810	Ph*	16.51(5) mag (Vega)
2015-11-03-11:57:41	Subaru	OIR	10800	Sp*	see Figure 3
2015-11-11-18:40:00	GMRT	1.4 GHz	22020	RI	< 0.07 mJy/beam

The start times, telescope name, observing band and observing duration are listed. In the fifth column time domain, radio imaging, photon counting, photometric and spectroscopic observations are denoted TD, RI, PC, Ph and Sp respectively, and detections (of either the FRB, fading transient or host galaxy) are denoted with an asterisk. The final column gives the detection level, or 3σ upper limits in the case of non-detections. 'Shadowing' refers to when the MWA was observing simultaneously with the Parkes telescope.